Ex-Vivo Ocular Perfusion Model to Study Vascular Physiology in the Mouse Eye

Ahmed M Eltanahy[1,*], **Cristian Franco**[1], **Priscilla Jeyaraj**[1], **Shipra Goswami**[1], **Elena Hughes**[1], **Albert L. Gonzales**[1,*]

[1]Department of Physiology and Cell Biology, University of Nevada School of Medicine, Reno, NV, 89557-0318, USA

Abstract

Several hypotheses have been tested to understand whole organ regulation in other organs such as the brain and kidney, but no such hypothesis has yet been proposed for ocular circulations. To some extent resolve this deficit our ex vivo mouse eye perfusion model takes the first step in elucidating the mechanisms controlling the individual components of the ocular circulation. Various isolated ocular vascular preparations have been utilized in studies of ocular vascular biology, physiology, and pharmacology, including studies on both normal and pathological conditions. However, there is still significant potential for further studies to improve our understanding of ocular circulation and its regulation. The choroid specifically is inaccessible to direct visualization due to the retina's high metabolic requirement with a transparency that cannot be compromised by an overly rich vascular network on the inner retinal side hindering the visualization of the choroid. In this technical paper, we provide a detailed description of all the steps to be followed from the enucleation of mouse eyes to cannulation of the ophthalmic artery and perfusion and Ex Vivo confocal microscopy imaging of the dynamic nature of the choroid circulation.

1. INTRODUCTION

The arterially perfused mammalian eye preparation is a multipurpose model for ophthalmology research. This preparation was pioneered at the National Eye Institute, NIH by (GOURAS and HOFF, 1970) and further refined by (Niemeyer, 1973). For these models, eyes from different mammalian species were used, with feline and bovine eyes being the most frequently encountered. In early work, the feline eye was utilized as a model to study the effect of the administration of pharmacological agents on photoreceptor functions (Sandberg et al., 1987). Similarly, Tazawa and Seaman studied the effects of anoxia and hypothermia on electroretinographic activity (Tazawa and Seaman, 1972). When performing these experiments, various parameters were monitored and controlled, including electroretinogram, intraocular pressure and arterial perfusion pressure (APP), glucose consumption, lactate dehydrogenase activity, oxygen consumption, and carbon dioxide production (Niemeyer, 1973, 2001; Pk et al., 2003; Su et al., 1995). Although

---

[*]**Address Correspondence To:** Albert L. Gonzales, Ahmed Eltanahy, University of Nevada School of Medicine, Department of Pharmacology, 11 Manville/MS-0352, Reno, NV 89557-0318, USA.

these studies increased our understanding of the intraocular drug delivery, photoreceptors and retinal electrophysiology, there is still significant potential for further studies to improve our understanding of ocular circulation and the choroid in particular. There is currently no technique that can directly study mechanisms regulating choroid blood flow, homeostasis, and physiology; therefore, we developed a mouse model of an *ex vivo* arterially perfused eye with the aim to address a lot of unanswered questions.

Mice are the most commonly used animal model for studying human disease. They are biologically very similar to humans and can be genetically manipulated to mimic virtually any human disease (Bryda, 2013). The choroid and retinal circulations in mice are structurally similar to that of humans (Nickla and Wallman, 2010). The choroid is the most vascular structure of the eye and has the highest blood flow per unit weight compared to any other tissue in the body (Lejoyeux et al., 2022). The choriocapillaris plays a critical role in supplying oxygen and nutrients to the photoreceptors and Retinal Pigment Epithelium (RPE). A high O_2 pressure (PO_2) is maintained by the unusually high flow rate in the choroidal circulation, which is necessary for providing enough O_2 and nutrients to the retina, which reaches its peak during the dark to maintain the dark current. Photoreceptors are depolarized in darkness requiring constant energy supply to power the Na^+/K^+ ATPase channels making them more energetic than almost any other cell type in darkness (Okawa et al., 2008) (Lejoyeux et al., 2022). Malfunction of choroidal circulation elicits many ophthalmological disorders. Diabetes, age-related macular degeneration (AMD), and glaucoma are just a few of the diseases that can cause alterations in the eye's vasculature and cause ocular circulation to malfunction (Kur et al., 2012; Lejoyeux et al., 2022). The presence of several genetic mouse models of ophthalmological diseases, including retinal degeneration; Pde6b[rd1], Rpe65r[d12], glaucoma; Nm2702, cone function loss; Cpfl and retinal vascular loss; Bmp4 (Chang et al., 2005), increases the importance for an *ex vivo* preparation to study the choroid blood flow.

The purpose of this work is to develop an experimental model to study and isolate the intrinsic vascular mechanisms regulating ocular blood flow, that is independent of neural input (Kur et al., 2012), and with the precise control of perfusion pressure and flow. Similar studies have used the ex-vivo vascular preparations to enhance our understanding of various mechanisms of autoregulation within microvascular, including; pressure-induced tone in the central nervous system (Klug et al., 2023), heart (Zhao et al., 2020) and skeletal muscle tissues (Haddy et al., 2006); capillary-mediated functional hyperemia in the brain and retina (Dabertrand et al., 2021; Longden et al., 2017; Thakore et al., 2021) vascular mechano-transduction (Davis et al., 2023), light signaling (Abbas et al., 2022) and immune-metabolic regulation of the vasculature (Hurley, 2021; Pan et al., 2021). The protocol provided will outline how to utilize the *ex vivo* pressurized mouse eye model, an experimental platform necessary for studying the vascular autoregulatory mechanism and ocular physiology in health and disease.

2. MATERIALS AND SUPPLIES

In Table 1, the vendors and catalog numbers of the supplies and tools used are listed with pictures included in the supplemental data (Table S1). In general, adult (2- to 3-month-old)

male B6-Albino mice (Jackson Laboratories, USA) were used. The reason for using non-pigment is that pigments in the choroid melanocytes will prevent imaging via a trans-scleral view. We are planning on developing a method of tissue clearing of the choroidal pigment and ex vivo live tissue imaging (Costantini et al., 2019; Lu et al., 2021). Surgical dissections were done under a binocular dissecting microscope with a 10x magnification. The eye was dissected in Ca^{2+}-free "Dissecting Solution" containing 119 mM NaCl, 3 mM KCl, 3 mM $MgCl_2$, 5 mM glucose, 26.2 mM $NaHCO_3$, and 1 mM sodium phosphate buffer, bubbled with 95% O_2/5% CO_2 (pH 7.4) at 4°C. During the experiment and data collection, the eye is continuously perfused with the Physiological Ocular Perfusate (POC) containing, DMEM/F-12 (Dulbecco's Modified Eagle Medium/Nutrient Mixture F-12) (ThermoFisher Scientific, 21041025) supplemented with 10% Fetal Bovine Serum (FBS) (Sigma).

3. DETAILED METHODS

This section a detailed description of the procedures followed for enucleation, dissection, cannulation of the ophthalmic artery, and *ex vivo* confocal microscopy imaging. For more details, videos and images recorded during the implementation of the protocol are included. The videos are entitled as follows:

Video S1: Dissection procedure of the Hemi-skull.

Video S2: Dissection procedure of the enucleated eye.

Video S3: Cannulation procedure of the ophthalmic artery.

3.1. Enucleation of mouse eyes

All the following procedures are done while maintaining the tissue with ice-cold and oxygenated dissecting buffer solution to decrease tissue metabolic activity. All procedures are following protocols approved by the University of Nevada, School of Medicine's Institutional Animal Care and Use Committee. Mice were deeply anesthetized with 4-5% isoflurane, decapitated, and heads were harvested and stored in an oxygenated and ice-cold dissecting solution. Fast eye enucleation directly after euthanasia (<30 minutes) is the best practice to maintain the preservation of the tissue and to avoid blood clotting or extended exposure of the tissue to Ca^{2+}-free conditions. The first step is to surgically dissect the skin from the skull. Using scissors, a longitudinal cut is made in the calvaria (Fig. 1a). The brain is dissected and flipped by cutting its attachments to the cranial nerves on the skull base. At this point, the skull is cut into two halves. An intact section of the whole optic and trigeminal nerves should be preserved (Fig 1c). Carefully cut the skull around the orbit and skull base using scissors. Dissect away any periocular tissue surrounding the eye inside the orbital cavity (muscles, connective tissues, etc.) and remove the attached periocular tissues from the anterior section of the eye (eyelids, Harderian gland, etc.). Attention should be paid to preserving a good length (~ 3 mm) of the artery feeding the Harderian gland for suturing to prevent leakage during pressurization. When blunt dissecting the Harderian gland, pay close attention not to cut this 3rd cranial nerve bundle (Fig 1- C&D) running along its superior border since it will cut right through the ophthalmic artery. For more details, please review video s1 and video s2.

3.2 Isolation of the ophthalmic artery and ligating of the branches.

A schematic representation of the main arteries within the ocular vascular network is shown in (Fig 2-A). The ophthalmic artery (diameter 200 uM) can be cannulated just proximal to the branching point of the short and long posterior ciliary arteries and the central retinal artery. Use the two micro-preparation forceps with a fine tip to carefully remove the connective and muscle tissues and isolate the ophthalmic artery (Video s2). The artery wall appears transparent and usually contains remaining red blood cells. Using 5 mm long nylon sutures, ligate the branches (~ 3 branches) coming off the ophthalmic artery branches and those supplying the Harderian gland. Note that the extraocular muscles are left intact so as not to disrupt the anterior ciliary circulation, however connective tissue adhering to the sclera can be carefully dissected away for better visualization of the choroid. For more details, please review video s2.

3.3 Preparation of the ophthalmic artery and cannulation

A glass pipette cannula with an Internal Diameter (ID) of .69 mm is pulled and attached to a custom-built 3D-printed pressurization chamber (table s1 & s2). The inner diameter of the tip of the cannula should be around the diameter of the ophthalmic artery in mice (~ 200 uM). For that purpose, the cannula's inner diameter should be around .69 mm. We use a pipette puller (Narishige Scientific Instrument PP-83) to taper the cannula's opening to be around the size of the ophthalmic artery (200 uM). The cannula is filled with oxygenated ice-cold POC solution while the pressurization chamber is filled with oxygenated ice-cold dissecting solution. It is important to ensure that no air bubbles are present in your cannula or tubing before cannulation. Prepare your sutures for cannulation. Cut the nylon thread into 5 mm pieces and place them on the sticky side of a double-sided tape on a Petri dish. Using a dissecting microscope, separate each piece into its filaments using fine forceps, and loosely prepare a simple half-hitch knot. Using fine forceps pull the suture into the bath solution, slide the knot onto the cannula and tighten it at a distance of 1 mm from the tip of the cannula. Repeat this process to have 2 sutures on the cannula. The dissected eye is then harvested in the chamber and the ophthalmic artery is cannulated and tied in place using two sutures (video s3). The eye globe is fixed to the tissue holder using 5 mm long pins to prevent microleakage, pay close attention, and keep the ophthalmo-ciliary artery straight and well-fixed to the cannula. For more details, please review video s3.

3.4 Perfusion of the eye

The pressurization chamber is immediately put under the confocal microscope. Using a peristaltic pump (table s1), oxygenated POC solution is circulated into the bath chamber to replace the dissecting solution while increasing the temperature to 37°C and gradually warming the eye over 30 mins. A pressure cannula is attached to a gravity column containing 37°C oxygenated POC solution which is then attached to the cannula inlet. To visualize the vasculature, 2 μL of isolectin B4 dye or FITC-dextran (1–12 mg/mL) is then loaded into the cannula inlet using a micropipette. Proper pressurization is confirmed by observing the flow of isolectin (using a 10x objective lens) inside the cannula and the choroid vessels without any leakage from the pressurization point or any of the arterial branches. Flow is maintained at 40 mmHg for 30 mins before collecting data by raising the

gravity column to the point where the pressure transducer measures 40 mmHg of perfusion pressure at the ophthalmic artery. Pressure changes are achieved either by lowering or increasing the height of the gravity column until reaching the perfusion pressure of interest. (Fig 3) shows a trans-scleral view of the mouse eye perfused with Isolectin or FITC-dextran.

3.5 Image Acquisition

Experiments were performed on a Crest Optics X-Light V3 spinning disk confocal and widefield microscope with 7 wavelength laser launch (LDI-7, 89 North) and dual ORCA-Fusion Gen-III sCMOS Cameras (Hamamatsu) on a Olympus (BX51WI) stand. 10 x objective lens is being used to confirm successful cannulation and visualization of the IB4. While a 60x objective lens can be used to obtain detailed images of the choroid vasculature. For a better depth of penetration of the light beam longer wavelength Griffonia Simplicifolia Lectin I (GSL I) IB4, 469 nm or 555 nm is utilized.

3.6 Flow dynamics experiments

Either microbeads 1 uM in diameter or FITC-Dextran 150 KD were injected into the cannula and perfused into the eye at different perfusion pressures (10:60 mmHg). Water immersive 40x objective lenses were used to image the dynamics of the flow using a spinning disk confocal microscope (Fig 3-4 & video s4 &s5).

3.7 Ex-Vivo Ca^{2+} imaging

Either cdh5-Gcamp6f mice or Fluo-4 am were used to study Ca2+ signaling in our ex-vivo preparation. 5 ul Fluo-4 am (3 uM) were injected in the ophthalmic artery through the cannula and the perfusion pressure was kept at zero mmHg for 20 minutes. And the perfusion pressure is resumed to gradually reach 40-50 mmHg. Spontaneous Ca2+ events were recorded using spinning disc confocal microscope at 470 nm of illumination.

4. POTENTIAL PITFALLS, AND TROUBLESHOOTING

The isolated eye technique has the advantage that the vasculature is intact and the relationship between the vasculature and the tissues that they supply is maintained (Niemeyer, 2001). Other advantages of perfusing mammalian eyes *ex vivo*: (i) control over the chemical input to the retina while excluding systemic inputs (ii) an opportunity to control arterial concentration and timing of externally applied pharmacology or metabolic molecules, (iii) access to retinal electrophysiology at several levels of information processing while simultaneously recording the optic nerve action potential along with modulating the ocular blood flow dynamics (Niemeyer, 2001; Rousou et al., 2019; Sandberg et al., 1987; Su et al., 1995). In Table 1, we summarize the results of our literature review on the research being done using isolated eye *ex vivo* perfusion techniques between 1970-2022. From the table results, there appears to be a lack of mice used as a model to perform the arterially perfused eye preparation which could be due to technical difficulties. The mouse has many similarities to humans in terms of anatomy, physiology, and genetics. The mouse genome is very similar to our own, making mouse genetic research particularly useful for the study of human diseases. Taken together, there is an immense need for us to re-visit this

technique considering the advancements in microscopy and vascular biology fields using the mouse eye model.

Multiple metabolic factors denote the experimental success rate. Lactic acidosis of the ocular tissues and the decrease in the bath solution's pH are major signs of tissue deterioration. Careful adjustment of the pH of the oxygenated perfusates contributes to the success of an experiment. For that reason, we use a handheld probe (Table S1) to test the pH of the perfusate and bath solution regularly during the experiment. It is also essential to adhere to a strict routine of cleaning the perfusion system after each experiment and leaving it filled with 70% ethanol in between experiments to prevent bacterial or fungal growth. In general, the preparation of this system is a process that requires training: the correct enucleation of the eyes, isolation of the ophthalmic artery, and cannulation. In the literature, there is a discrepancy regarding the duration of time between animal termination and the enucleation of the eyes. In the study of (Gilger et al., 2013) pig eyes were enucleated after animal euthanasia and were cannulated within 15 min, while in the study of (GOURAS and HOFF, 1970) cat eyes were cannulated 3–10 min after euthanasia. In other studies where bovine eyes were used, the authors report blood vessel cannulation 1 h: 2 h after animal termination (Koeberle et al., 2006; Trap et al., 2009). With mice, we recommend enucleation within 30 mins after euthanasia to prevent endothelial damage and long exposures of the ocular circulation to Ca^{2+}-free conditions. In addition, in the case that the isolation of the ophthalmic artery takes an excessive amount of time, it is important to keep the tissue in a continuously oxygenated and ice-cold dissecting solution.

Another important point is the ligation of all blood vessels coming from the ophthalmic artery including those supplying the Harderian gland. If the preserved part of the ophthalmic artery is not long enough for cannulation and it is too proximal to the branching point of ciliary and the central retinal arteries, it is advised not to continue, but rather move to another eye. In that case, the sections of tissues perfused by the long and short posterior ciliary arteries (e.g., choroid, iris, and ciliary body) will not be pressurized and retinal tissue viability will be diminished in case of prolonged perfusion experiments. If perfusion is tested but Isolectin is not visible in the choroidal blood vessels, then most likely there is a leakage at the ophthalmic artery; a branch is not ligated; a bend is present in the artery, or the cannula is clogged by the surrounding tissue or salts build up inside its tip. It is anticipated to experience varying degrees of vascular leakage during perfusion. Leaks can be difficult to identify, but they can be visualized using confocal microscopy with a fluorescent dye, like Isolectin or dextran. Also, When the vortex vein near the equator on the lower surface of the mouse eye is released and not blocked against the eye's holder, perfusion should improve as it prevents the buildup of abnormal pressures of the perfusate in the uveal circulation.

A healthy ultrastructure of the retina is dependent on the flow rate in this perfusion system. It is critical not to perfuse the eye under high flow for a prolonged period. Reme and Niemeyer (Reme´ and Niemeyer, 1975) performed light and electron microscopy studies on eyes that underwent high flow perfusions showing that at high flow rates patches of cystic changes (vacuoles) in the RPE were observed initiating retinal detachments which could be due to increased exudation across the choriocapillaris endothelium. Using

electron microscopy, they showed higher percentages of adverse cellular changes in the retina in inverse proportion to the flow rate of perfusion in the cat's eyes. Another limitation of the system described is that it only consists of an inlet (cannulation of the ophthalmic artery), with the venous drainage (outflow) being free. Therefore, the perfused substances are not re-circulated. If a closed system is required, the eye can be placed in a container in which all outflow fluids can be collected for analysis. The duration of tissue viability when physiological buffers are perfused can be evaluated over time with various methods, depending on the specific application. Some examples are: (i) activity of lactate dehydrogenase (LDH), (ii) measurement of the blood (or perfused solution) flow using confocal microscopy, (iii) measurement of the intra-ocular pressure (IOP), and (iv) histological evaluation of tissue deterioration.

5. Maintenance of Choroidal Flow Dynamics in the arterially perfused eye.

Most of the retina's oxygen is consumed by the highly metabolically demanding photoreceptors provided by the choriocapillaris (Lejoyeux et al., 2022). A steep gradient of oxygen tension is necessary to achieve a high oxygen transport, and this gradient is maintained by the high blood flow in the choroid, the highest of any tissue in the body per unit tissue weight (Lejoyeux et al., 2022; Nickla and Wallman, 2010). A reduction in the mean arterial blood pressure and accordingly choroid blood flow was shown to reduce the O_2 content in the choroid suggesting that at low perfusion pressures there is hypoxia/anoxia in some tissue supplied by the choroidal/uveal vessels, despite a relatively well oxygenated venous blood (Alm and Bill, 1970). We also found that at low perfusion pressures, there are capillaries in the choroid that could lose their supply/perfusion (Fig-3 E&F) & Video S5). Therefore, adequate perfusion pressure in the isolated eye is critical for the success of this experiment and proper nourishment of the outer retina.

Mural cells, including vascular smooth muscle cells (SMCs) and capillary pericytes control the perfusion of the microcirculation. Three subtypes of pericytes have been characterized (Hartmann et al., 2022) within the capillary system. Beginning at the most proximal region to the feeding arteriole, or within the arteriole-to-capillary transition zone (Ratelade et al., 2020), are ensheathing pericytes, which have extensive, densely packed projections that wrap around capillary segments (Gonzales et al., 2020). Deeper into capillary network pericytes transition into mesh and thin-stranded subtypes, which are morphologically different distinct with long processes that can extend to cover 100's of microns along the capillary vessel. To study the presence of these cells in the choroid circulation, we used albino NG2-dsRed (Mural Cell reporter) mice to study the structure and morphological heterogeneity of mural cells in our arterially perfused eye model (Fig 2 &3). Unlike the retinal vasculature, whereby the ensheathing pericytes within in the transition region, or branch order of 3.8 ± 0.3 branches (Gonzales et al., 2020; Klug et al., 2023), the choroid circulation has a short transition segment (Fig 3) with an average branch order of 1.6 ± 0.7 branches (n= 12). The transition zone has been proposed to be important in regulating blood flow entering the capillary network, therefore, as previously described (Zouache et al., 2016), the short transition segments in the choroid may play an important role maintaining a high blood flow system. We also found that there is a heterogenous organization of the choriocapillaris showing finger-like and maze-like patterns in the peripheral choroid, while

showing honeycomb appearance in the central part (Fig 3, B-D). Similar results have been reported in the literature (Zaitoun et al., 2022). Functional imaging of the choroid is a very under studied area in ophthalmology research. For that purpose, we used our *ex vivo* eye preparation to image spontaneous Ca^{2+} dynamics in endothelial cells using membrane permeable Ca^{2+} indicators, Fluo-4 am or cdh5-Gcamp6f (Fig 3E). It will be also interesting to study vascular cell Ca^{2+} dynamics and homeostasis in response at different perfusion pressures and in mice models of retinal degeneration and ageing.

The flow dynamics in the choriocapillaris is a very under-studied area in ophthalmology research due to technical difficulties. As a result of certain clinical and morphological observations (Hayreh, 2004), some authors have assumed that there are segmentally arranged arteriolar and capillary units that are independent of one another to a certain extent describing the choroid as an end-arterial circulatory system (Lee et al., 2017; Singh Hayreh, 1974). This hypothesis was, however, doubted by several studies (Lee et al., 2017; Singh Hayreh, 1974). We used 150 KD dextran and 1uM-sized beads to re-visit the flow dynamics of the choroid circulation. We found that the choroid arterioles run in relatively delimited sectors of the choriocapillaris without forming anastomoses with their neighboring branches before their final division. However, the choriocapillaris network appears to have continuity by inter-capillary anastomoses, and certain sectors do have alternative blood supply (Fig 4 & video s4). In the future, we are hoping to extend this technique to permit selective perfusion and hence characterization of the microvascular responses of the retinal and choroidal circulations.

6. CONCLUSION

It has been shown that under adequate arterial perfusion an isolated mammalian eye can maintain structural integrity and physiological performance similar to *in vivo* studies. Here we reported a detailed description of the method for arterial perfusion of mouse eyes supported by images and videos. It is necessary to create new isolated vascular preparations and methods for researching the physiology and pharmacology of the various orders of choroidal vasculature. Such isolated ocular vascular preparations will enable further research into the pathophysiology of ocular vascular illnesses, examination of the etiology of normal vascular biology, and ultimately support the development of novel therapeutic approaches.

Supplementary Material

Refer to Web version on PubMed Central for supplementary material.

ACKNOWLEDGEMENTS

REFERENCES

Abbas F, Becker S, Jones BW, Mure LS, Panda S, Hanneken A, Vinberg F, 2022. Revival of light signalling in the postmortem mouse and human retina. Nature 606, 351–357. [PubMed: 35545677]

Alm A, Bill A, 1970. Blood Flow and Oxygen Extraction in the Cat Uvea at Normal and High Intraocular Pressures. Acta Physiologica Scandinavica 80, 19–28. [PubMed: 5475327]

Bryda EC, 2013. The Mighty Mouse: the impact of rodents on advances in biomedical research. Missouri medicine 110, 207–211. [PubMed: 23829104]

Chang B, Hawes NL, Hurd RE, Wang J, Howell D, Davisson MT, Roderick TH, Nusinowitz S, Heckenlively JR, 2005. Mouse models of ocular diseases. Visual Neuroscience 22, 587–593. [PubMed: 16332269]

Costantini I, Cicchi R, Silvestri L, Vanzi F, Pavone FS, 2019. In-vivo and ex-vivo optical clearing methods for biological tissues: review. Biomedical optics express 10, 5251–5267. [PubMed: 31646045]

Dabertrand F, Harraz OF, Koide M, Longden TA, Rosehart AC, Hill-Eubanks DC, Joutel A, Nelson MT, 2021. PIP$_2$ corrects cerebral blood flow deficits in small vessel disease by rescuing capillary Kir2.1 activity. Proceedings of the National Academy of Sciences 118, e2025998118.

Davis MJ, Earley S, Li Y-S, Chien S, 2023. Vascular mechanotransduction. Physiological Reviews 103, 1247–1421. [PubMed: 36603156]

Gilger EMA, Jacklyn HS, Brian C, 2013. Effect of Choroidal Perfusion on Ocular Tissue Distribution After Intravitreal or Suprachoroidal Injection in an Arterially Perfused Ex Vivo Pig Eye Model. https://home.liebertpub.com/jop.

Gonzales AL, Klug NR, Moshkforoush A, Lee JC, Lee FK, Shui B, Tsoukias NM, Kotlikoff MI, Hill-Eubanks D, Nelson MT, 2020. Contractile pericytes determine the direction of blood flow at capillary junctions. Proceedings of the National Academy of Sciences of the United States of America 117, 27022–27033. [PubMed: 33051294]

GOURAS P, HOFF M, 1970. Retinal Function in an Isolated, Perfused Mammalian Eye. Investigative Ophthalmology & Visual Science 9, 388–399.

Haddy FJ, Vanhoutte PM, Feletou M, 2006. Role of potassium in regulating blood flow and blood pressure. American Journal of Physiology-Regulatory, Integrative and Comparative Physiology 290, R546–R552. [PubMed: 16467502]

Hartmann DA, Coelho-Santos V, Shih AY, 2022. Pericyte Control of Blood Flow Across Microvascular Zones in the Central Nervous System. Annual Review of Physiology 84, 331–354.

Hayreh SS, 2004. Posterior ciliary artery circulation in health and disease: the Weisenfeld lecture. Invest Ophthalmol Vis Sci 45, 749–757; 748. [PubMed: 14985286]

Hurley JB, 2021. Retina Metabolism and Metabolism in the Pigmented Epithelium: A Busy Intersection. Annual review of vision science 7, 665–692.

Klug NR, Sancho M, Gonzales AL, Heppner TJ, O'Brien RIC, Hill-Eubanks D, Nelson MT, 2023. Intraluminal pressure elevates intracellular calcium and contracts CNS pericytes: Role of voltage-dependent calcium channels. Proceedings of the National Academy of Sciences 120, e2216421120.

Koeberle MJ, Hughes PM, Skellern GG, Wilson CG, 2006. Pharmacokinetics and Disposition of Memantine in the Arterially Perfused Bovine Eye. Pharmaceutical Research 23, 2781–2798. [PubMed: 17103338]

Kur J, Newman EA, Chan-Ling T, 2012. Cellular and physiological mechanisms underlying blood flow regulation in the retina and choroid in health and disease. Progress in Retinal and Eye Research 31, 377–406. [PubMed: 22580107]

Lee JE, Ahn KS, Park KH, Pak KY, Kim HJ, Byon IS, Park SW, 2017. Functional end-arterial circulation of the choroid assessed by using fat embolism and electric circuit simulation. Scientific Reports 7, 2490. [PubMed: 28559567]

Lejoyeux R, Benillouche J, Ong J, Errera MH, Rossi EA, Singh SR, Dansingani KK, da Silva S, Sinha D, Sahel JA, Freund KB, Sadda SR, Lutty GA, Chhablani J, 2022. Choriocapillaris: Fundamentals and advancements. Prog Retin Eye Res 87, 100997. [PubMed: 34293477]

Longden TA, Dabertrand F, Koide M, Gonzales AL, Tykocki NR, Brayden JE, Hill-Eubanks D, Nelson MT, 2017. Capillary K(+)-sensing initiates retrograde hyperpolarization to increase local cerebral blood flow. Nature neuroscience 20, 717–726. [PubMed: 28319610]

Lu W, Pei Z, Hu W, Tan C, Tong X, Feng Y, Sun X, 2021. Recent progress in optical clearing of eye tissues. Experimental Eye Research 212, 108796. [PubMed: 34662543]

Nickla DL, Wallman J, 2010. The multifunctional choroid. Prog Retin Eye Res 29, 144–168. [PubMed: 20044062]

Niemeyer G, 1973. ERG dependence on flow rate in the isolated and perfused mammalian eye. Brain Research 57, 203–207. [PubMed: 4716752]

Niemeyer G, 2001. Retinal Research using the Perfused Mammalian Eye. Progress in Retinal and Eye Research 20, 289–318. [PubMed: 11286895]

Okawa H, Sampath AP, Laughlin SB, Fain GL, 2008. ATP consumption by mammalian rod photoreceptors in darkness and in light. Current biology : CB 18, 1917–1921. [PubMed: 19084410]

Pan WW, Wubben TJ, Besirli CG, 2021. Photoreceptor metabolic reprogramming: current understanding and therapeutic implications. Communications Biology 4, 245. [PubMed: 33627778]

Pk Y, Y.D., Su EN, Cringle SJ, Yu, 2003. Isolated preparations of ocular vasculature and their applications in ophthalmic research. Progress in retinal and eye research 22.

Ratelade J, Klug NR, Lombardi D, Angelim M, Dabertrand F, Domenga-Denier V, Al-Shahi Salman R, Smith C, Gerbeau JF, Nelson MT, Joutel A, 2020. Reducing Hypermuscularization of the Transitional Segment Between Arterioles and Capillaries Protects Against Spontaneous Intracerebral Hemorrhage. Circulation 141, 2078–2094. [PubMed: 32183562]

Reme C, Niemeyer G.n., 1975. Studies on the ultrastructure of the retina in the isolated and perfused feline eye. Vision Research 15, 809–IN807. [PubMed: 1154660]

Rousou C, Hoogenboom P, van Overdam KA, Storm G, Dorrestijn J, Mastrobattista E, 2019. A technical protocol for an experimental ex vivo model using arterially perfused porcine eyes. Experimental Eye Research 181, 171–177. [PubMed: 30735657]

Sandberg MA, Pawlyk BS, Crane WG, Schmidt SY …, 1987. Effects of IBMX on the ERG of the isolated perfused cat eye.

Singh Hayreh S, 1974. The choriocapillaris. Albrecht von Graefes Archiv für klinische und experimentelle Ophthalmologie 192, 165–179. [PubMed: 4219556]

Su E-N, Yu D-Y, Alder VA, Yu PK, Cringle SJ, 1995. Altered vasoactivity in the early diabetic eye: Measured in the isolated perfused rat eye. Experimental Eye Research 61, 699–711. [PubMed: 8846842]

Tazawa Y, Seaman A, 1972. The electroretinogram of the living extracorporeal bovine eye. The influence of anoxia and hypothermia. Investigative Ophthalmology & Visual Science 11, 691–698.

Thakore P, Alvarado MG, Ali S, Mughal A, Pires PW, Yamasaki E, Pritchard HAT, Isakson BE, Tran CHT, Earley S, 2021. Brain endothelial cell TRPA1 channels initiate neurovascular coupling. eLife 10, e63040. [PubMed: 33635784]

Trap F.A.M.d.C., Bernard AZ, Nico H, 2009. Prolonged normothermic perfusion of the isolated bovine eye: initial results. 10.3109/02713689308999453.

Zaitoun IS, Song YS, Zaitoun HB, Sorenson CM, Sheibani N, 2022. Assessment of Choroidal Vasculature and Innate Immune Cells in the Eyes of Albino and Pigmented Mice. Cells 11.

Zhao G, Joca HC, Nelson MT, Lederer WJ, 2020. ATP- and voltage-dependent electro-metabolic signaling regulates blood flow in heart. Proceedings of the National Academy of Sciences 117, 7461–7470.

Zouache MA, Eames I, Klettner CA, Luthert PJ, 2016. Form, shape and function: segmented blood flow in the choriocapillaris. Scientific Reports 6, 35754. [PubMed: 27779198]
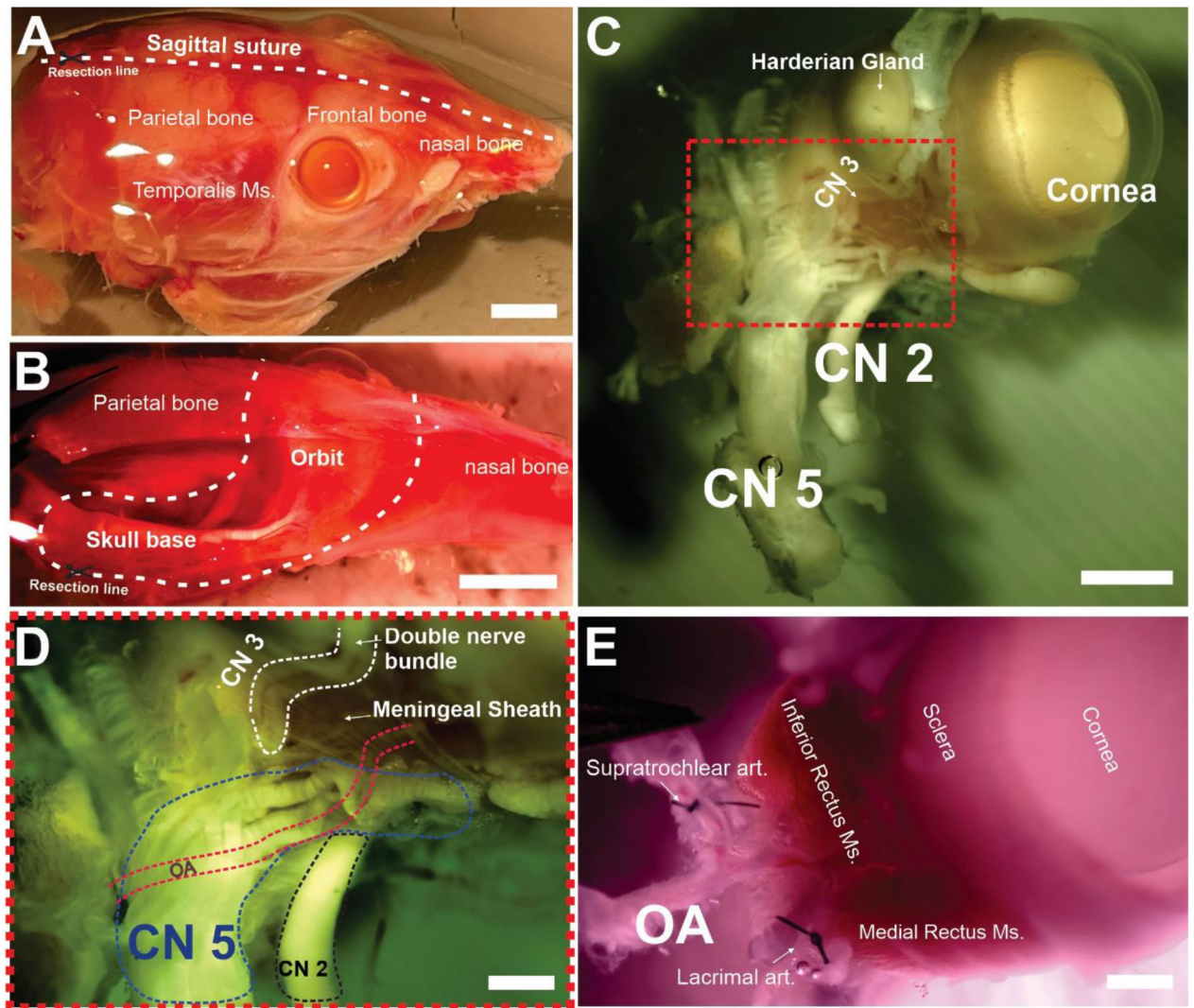
Figure 1. Microdissection steps of the Ophthalmic Artery.
After euthanasia, the skin is dissected from the skull (A) a longitudinal incision is made along the sagittal suture to yield a hemi-section of the skull (B) The orbital bone is carefully cut along the dashed line to separate the eyeball and its surround soft tissue (Video S1) (C). (D&E) Be careful not to dissect the double nerve bundle running along the medial border of the harderian gland (CN3) and the nervous tissue should be dissected with care to yield the isolated eye with its vascular supply intact starting from the ophthalmic artery. The dashed red lines in (D) represent the anatomical localization of the ophthalmic artery beneath the cranial nerves. (E) Shows the ligated axillary branches of the ophthalmic artery, The Extraocular Muscles (EOMs) are left intact. CN2 = 2nd cranial nerve, CN3 = 3rd cranial nerve, CN5= 5th cranial nerve. OA= Ophthalmic artery. Scale Bars: A & B= 2 mm, C= 1 mm, D&E= 500 uM.
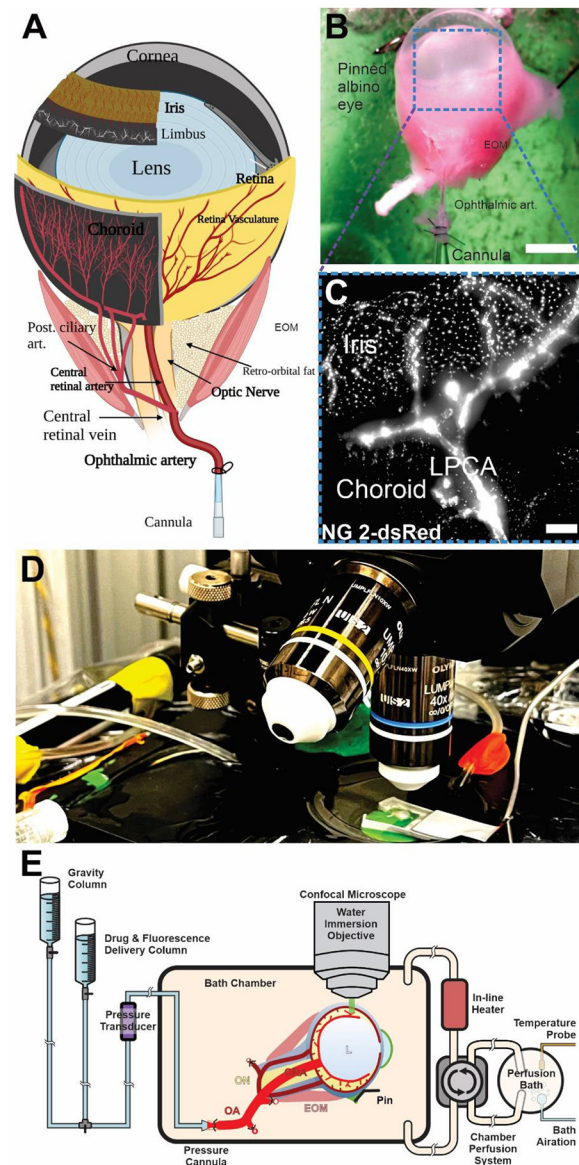
Figure 2. Cannulation of the Ophthalmic Artery and experimental setup.
Anatomical illustration of the isolated mouse eye with its blood supply and cannulation
point (A&B). (C) 10x imaging of an arterially perfused NG2-dsRed albino eye via
a transscleral view, refer to video S6 for z stack rendering and intravascular lectin
perfusion. (D&E) Experimental setup for ex-vivo confocal microscopy imaging setup
showing an enucleated and arterially cannulated eye superfused with oxygenated and
37° C Physiological Ocular Perfusate buffer (Refer to table S1&S2 for supporting
information). ON, Optic Nerve; CRA, Central Retinal Artery; EOM, Extraocular Muscles;
OA, Ophthalmic artery; LPCA, Long Posterior Ciliary Artery; PCA, Posterior Ciliary
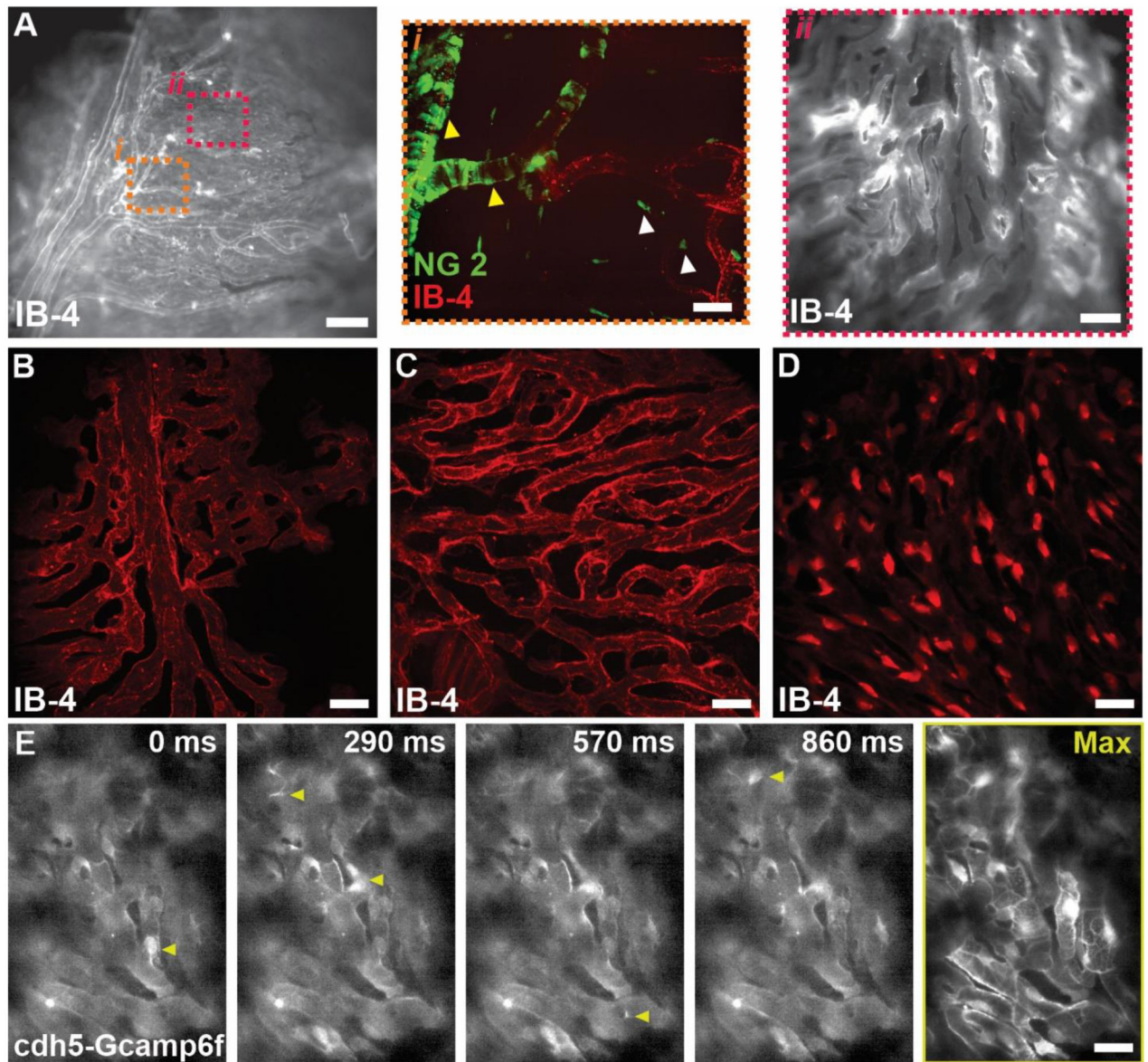Arteries; ACA, Anterior Ciliary Artery.

Figure 3. Structural and functional imaging of the choroid circulation.
(A) Isolectin perfused ex vivo eye preparation using 10x magnification (A) 60x magnification (i&ii). (B-D) Representative images (of 10 images for each group) classifying the structural heterogeneity of the choriocapillaris; finger-like pattern (B), maze-like pattern (C) and honeycomb like pattern (D) in the lectin perfused ex-vivo eye. Scale Bars: A= 200 μm, i&ii= 25 μm. (E) Ex-vivo functional Ca^{2+} imaging of the choriocapillaris showing spontaneous Ca^{2+} events (yellow arrowheads) using cdh5-Gcamp6f in our ex-vivo preparation (refer to Video S7). Scale Bar: B-D= 25 μm, E= 15 μm. IB4, Isolectin B4, SMCs= Smooth Muscle Cells.
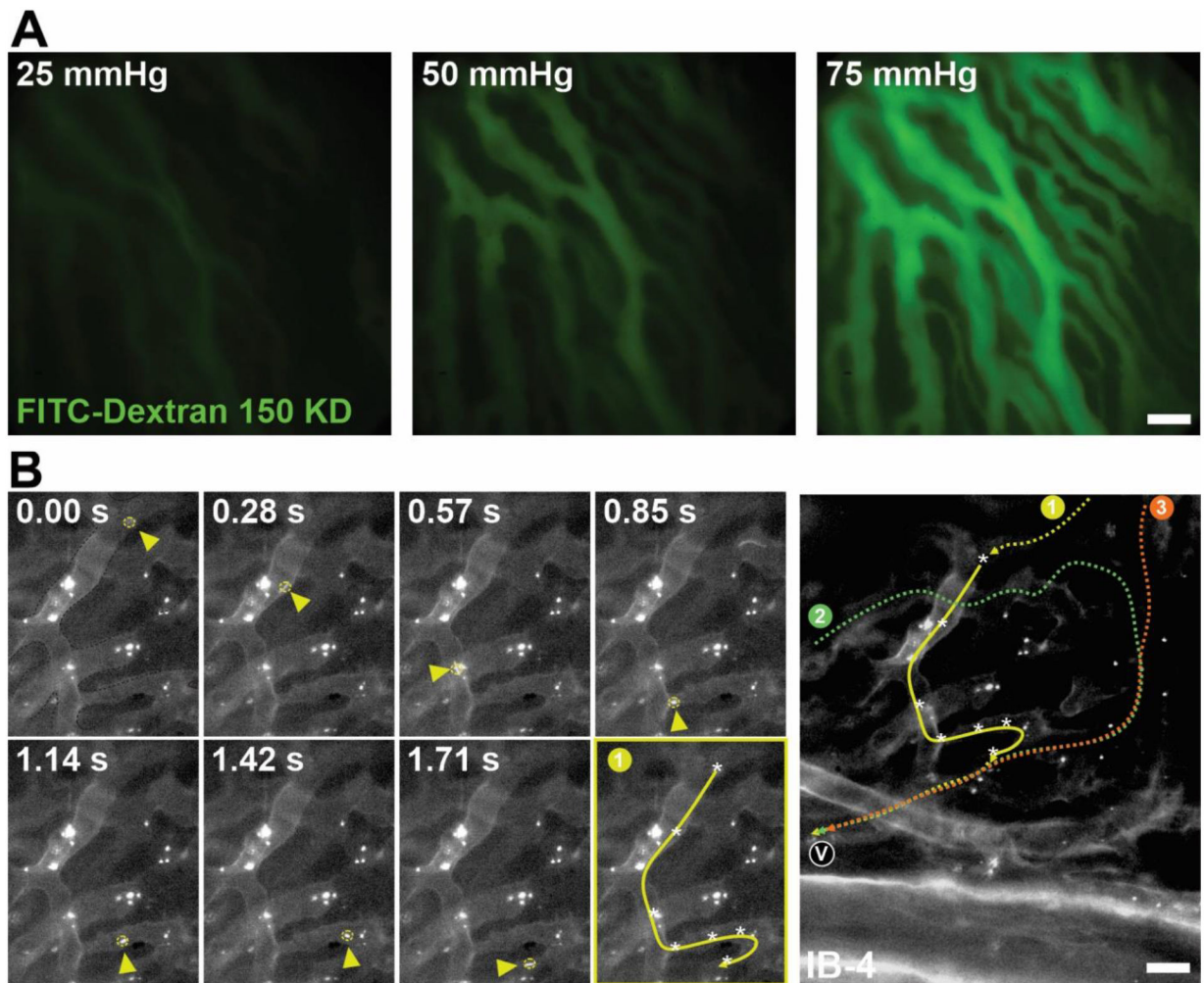
Figure 4. Flow dynamics of the choriocapillaris.

(A) Representative images of the perfusion of 150 KD FITC-dextran in choriocapillaris in the arterially perfused ex vivo preparation. Flow of FITC-dextran increased at increasing perfusion pressures. Scale Bar: 20 μm. (B) Representative time-lapse images and bead tracking path summary (1, yellow) of a flowing 1μm fluorescent bead (yellow arrowhead and dashed circle) through the choriocapillaris. When tracking three separate beads entering the region of interests, we observed that the beads entered the capillary network from different vessels (1, 2, and 3) but exited through the same venule (v) suggesting that the presence of inter-capillary anastomosis. Scale Bar: 25 μm. (Refer to Video S4&S5).

Table 1.

Literature Review (1970:2022) isolated mammalian eye preparations.

Species	Studied Parameter	Reference
Cat	Electroretinography	Gouras and Hoff (1970)
	Electroretinography	Niemeyer (1973)
	Electrophysiology	Nelson et al. (1975)
	Pharmacological testing	Schneider and Zrenner (1985)
	Electroretinography	Alder et al. (1986)
	Electroretinography & vascular physiology	Cringle et al. (1986,1987,1988)
	Electroretinography	Sandberg et al. (1987)
	Electroretinography	Thoreson and Purple (1989)
	Electroretinography	Peachey et al. (1993)
	Retinal Electrophysiology	Freed and Nelson (1994)
	Pharmacological testing	Macaluso, et al. (2003)
	Electroretinography	Kuze et al. (2003)
Rat	Vascular physiology	Su et al. (1995)
	Retinal Oxygen	Yu et al. (2000)
Squirrel	Photoreceptor electrophysiology	Leeper et al. (1985)
Dog	Electrophysiology	Niemeyer (1983)
Rabbit	Spectral interactions	de Monasterio (1978)
	Ocular blood flow and Intraocular Pressure	Pinxteren et al. 1984, 1985
	Electroretinography, pharmacological agents and vascular physiology	Shahidullah et al. 2003,2005
	Vascular physiology	delgado et al. 2009
Bovine	Pharmacokinetics	Tazawa and Seaman (1972)
	Electroretinography	J C Millar et al. (1997)
	Electroretinography	Koeberle et al. 2006
	Aqueous formation & Electroretinography	A J McNeish et al. 2001, 2002
Guinea pig	Intraocular pressure, ocular vasculature	Cringle et al. (1997)
Monkey	Intraocular pressure (IOP), aqueous humor formation	Schuurmans and Zrenner (1981)
Pig	Photoreceptor physiology	R Townsend et al. 2006
	Vascular physiology	Jun et al. 2009
	Electroretinography	Yiu-Fai Ng et al. 2008
	Drug delivery and clearance	Abarca et al. 2013
	Technical protocol	Rousou et al. 2019
Sheep	Electroretinography	Mains et al 2011, Mains et al. 2012